The Electrochemical Society
Advancing solid state & electrochemical science & technology

Analysis of EIS Technique and Nafion 117 Conductivity as a Function of Temperature and Relative Humidity

View the article online for updates and enhancements.

Analysis of EIS Technique and Nafion 117 Conductivity as a Function of Temperature and Relative Humidity

Rameshwar Yadav and Peter S. Fedkiw*,z

North Carolina State University, Raleigh, North Carolina 27695, USA

This work presents an analysis of electrochemical impedance spectroscopy (EIS) technique and conductivity of Nafion 117 membrane at relative humidities of 10–100% and at temperatures 25–80°C. A correlation is presented to calculate the conductivity of Nafion 117 over the temperature and water vapor activity range measured. The correlation also captures the effect of water vapor activity on the activation energy for proton transport. The two-probe EIS technique was employed to measure the in-plane membrane resistance and the effect of platinum electrode dimension was investigated. An equivalent circuit that captures the impedance spectra was used to resolve the ionic resistance. The capacitive behavior of Nafion 117 with water-uptake was observed and analyzed. The two- and four-probe methods are compared and yield essentially identical Nafion 117 conductivities (two-probe $79 \pm 1\%$ mS cm^{-1}, four-probe $82 \pm 1\%$ mS cm^{-1}) in room-temperature liquid water.
© 2012 The Electrochemical Society. [DOI: 10.1149/2.104203jes] All rights reserved.

Ionic conductivity of a polymer electrolyte membrane (PEM) is of paramount significance since it affects the ohmic loss in fuel cells. Nafion 117 possesses the benchmark conductivity for comparison of new PEM candidates. Many studies have reported Nafion 117 ionic conductivity, and even at the same condition of temperature and water activity, the results vary.[1–18] The characterization of new PEMs requires use of consistent methods to obtain agreeable results of Nafion 117 conductivity.

Generally, the electrochemical impedance spectroscopy (EIS) technique with a two- or four-probe method is employed to extract the ionic resistance from an equivalent circuit model of the PEM. In the two-probe method, interpretation of low-ionic resistance from impedance spectra can be challenging because the PEM-electrode interfacial impedance can obscure the PEM impedance. However, the two-probe method can be suitable for high-ionic resistance membrane. The four-probe method can separate interfacial contact impedance and is appropriate for low-ionic resistance, but this method requires more sophisticated equipment than the two-probe method. In the four-probe method, measurements in certain frequency range can produce impedance spectra free from artifacts. It is also essential to eliminate artifacts in impedance spectra from the four-probe method to obtain conductivity that is identical with that from the two-probe method.

Many publications report Nafion 117 ionic conductivity at various water content and temperatures.[1–18] Because of different measurement techniques, Nafion 117 conductivity varies significantly at identical measurement conditions of membrane history, treatment protocol, temperature, and water content (Table I, Refs. 1–18). For example, Nafion 117 conductivity at 20°C is reported to vary from 63 to 90 mS cm^{-1} in liquid water and from 51 to 96 mS cm^{-1} at 100% relative humidity.[1–6] Nafion 117 conductivity increases with relative humidity and temperature. However, it was reported that Nafion 117 conductivity reaches a maximum at 60°C in the temperature range of 25–100°C.[9,10] Sone et al. also report that conductivity decreased with temperature from 20 to 45°C and increased with temperature from 45 to 80°C for a given relative humidity.[6] Apparently, there is a lack of comprehensive and agreeable results on Nafion 117 conductivity at PEM fuel cells operating conditions ranging from 10 to 100% relative humidity and 25 to 80°C temperature.

Many perceive that through-plane ionic conductivity is representative of proton conduction in an actual fuel cell. Conventionally, an in-plane conductivity measurement is preferred over a through-plane measurement because, for fixed ionic conductivity, dimensions of the PEM used in the conductivity cell can be adjusted to obtain a measurable ionic resistance with the EIS technique. In the through-plane configuration, for a fixed area of electrodes, the PEM thickness acting as inter-electrode distance sets the ionic resistance, which is typically too low to measure by the EIS technique.

Extrapolation of the semi-circle arc or the low-frequency linear spectra on a Nyquist plot to the real-axis yields the ionic resistance. In a typical Nyquist plot, a change in shape and magnitude of impedance spectra occurs because of impedance variation with water uptake and temperature. A single equivalent circuit that can capture the impedance at different water content and temperature can be useful for ionic conductivity measurement.

Distortion in the impedance spectra will lead to a misinterpretation of PEM ionic resistance. A uniform current distribution at the PEM-electrode interface can produce distortion-free impedance spectra resulting in improved ionic conductivity measurement. An excessive contact area at the PEM-electrode interface can lead to non-uniform current distribution resulting in distortion of impedance spectra. Reduction in contact area can provide a more uniform current distribution and attenuate the distortion in impedance spectra. The EIS technique can also be applied to study the change in dielectric properties of PEM due to water uptake. PEM capacitance is dependent on water content because of the high-dielectric constant of water (79).[19,20] As a result, the PEM impedance and time-constant (RC) will vary. For a fixed dimension of PEM, this variation appears as change in shape and magnitude of PEM impedance spectra.

Conductivity measurement requires good control of relative humidity and temperature. Use of a dynamic flow system of wet and dry gases to control the relative humidity requires expensive apparatus, good flow control, accurate humidity sensor, and can be cumbersome. A simple method to control RH, however, is the equilibration of vapor above aqueous salt solutions such as lithium chloride. Because of strong variation of liquid water activity with salt concentration, control of relative humidity in any custom-built enclosure can be achieved effectively with aqueous lithium chloride salt solutions.[21–23]

This work presents an analysis of the EIS technique for conductivity measurement of Nafion 117 as a function of relative humidity and temperature. An equivalent circuit that encompasses the impedance spectra at all measurement conditions is described. Advantages of in-plane conductivity measurement and challenges associated with through-plane conductivity measurement are critically analyzed and discussed. For fixed ionic conductivity, effect of electrode area on through-plane resistance is analyzed.

Experimental

An apparatus based on ASTM E104-02 was employed to measure the ionic conductivity of a PEM as function of relative humidity and temperature.[24] Ratio of headspace volume to active surface area of salt solution was set to be below 25 cm.[24] The apparatus consists of a glass vessel with a detachable cover. Six PEM-sample holders were

Table I. Nafion 117 Ionic Conductivity.

| T (°C)	Phase	Cond. (S/cm)	EIS Method	Pretreatment Method	Ref.
20	Liquid	0.063	2P, TP	H_2O_2, HCl (2M), 0.5 hr	1
	Liquid	0.077	2P, IP	H_2O_2, HCl (2M), 0.5 hr	1
	Liquid	0.090	2P, TP	HNO_3 (33 wt%), 2 hr	2
	Vapor (93%)	0.014	CP, IP	HNO_3 (30 wt%), 0.5 hr	3
	Vapor (92%)	0.036	2P	H_2O_2, H_2SO_4 (0.5M), 1 hr	4
	Vapor	0.051	2P	H_2O_2, H_2SO_4 (0.5M), 1 hr	4
	Vapor	0.055	4P, IP	H_2O_2, HCl (5 wt%), 1 hr	5
	Vapor	0.066	CP, IP	HNO_3 (30 wt%), 0.5 hr	3
	Vapor	0.096	4P, IP	H_2O_2, H_2SO_4 (0.5M), 1 hr	6
23	Liquid	0.090	4P, IP	N/D	7
25	Liquid	0.048	2P, TP	H_2O_2, HNO_3 (20 wt%), 1 hr	8
	Vapor	0.061	2P, IP	HNO_3 (3M)	9
	Vapor (98%)	0.075	4P, IP	NA	10
30	Liquid	0.087	2P, IP	H_2O_2, H_2SO_4 (0.5M), 1 hr	11
	Liquid	0.100	2P, IP	H_2O_2, H_2SO_4 (0.5M), 1 hr	12
	Vapor (95%)	0.019	2P, IP	H_2O_2, H_2SO_4 (1M), 1 hr	13
	Vapor (95%)	0.047	4P, IP	HNO_3 (32 wt%), 1 hr	13
	Vapor (90%)	0.062	4P, IP	NA	14
	Vapor	0.062	2P, IP	H_2O_2, H_2SO_4 (0.5M), 1 hr	12
45	Vapor	0.045	4P, IP	H_2O_2, H_2SO_4 (0.5M), 1 hr	6
50	Vapor	0.112	2P, IP	HNO_3 (3M)	9
	Vapor	0.135	4P, IP	H_2O_2, H_2SO_4 (0.5M), 1 hr	11
65	Liquid	0.079	2P, TP	H_2O_2, HNO_3 (20 wt%), 1 hr	8
70	Vapor	0.071	4P, IP	H_2O_2, H_2SO_4 (0.5M), 1 hr	6
75	Vapor (95%)	0.034	2P, TP	NA	15
80	Vapor	0.105	2P, TP	NA	16
90	Liquid	0.184	2P, IP	H_2O_2, H_2SO_4 (0.5M), 1 hr	17
	Vapor (98%)	0.061	4P, IP	NA	10
	Vapor (95%)	0.020	2P, IP	HNO_3 (32 wt%), 1 hr	13
	Vapor (95%)	0.072	4P, IP	HNO_3 (32 wt%), 1 hr	13
95	Liquid	0.025	2P, TP	HNO_3 (3M)	18
	Vapor (98%)	0.033	2P, TP	HNO_3 (3M)	18
	Vapor	0.081	2P, IP	HNO_3 (3M)	9

[a] 2P-two-probe method, 4P-four-probe method, IP-in-plane configuration, TP-through-plane configuration, CP-coaxial-probe method, Vapor-100% relative humidity, and Liquid-liquid water.

attached to a perforated ceramic plate onto which conductivity cells were fixed. A hygrometer (Fisher Scientific) displayed the relative humidity and temperature. A tapered hole at the center of the top cover allowed twelve wires to pass through a silicone rubber stopper for electrical contact. A needle valve in the top cover allowed control of atmospheric pressure in the system.

Fig. 1 shows a schematic of a typical conductivity cell. The cells were made of Kel-F (polychlorotrifluoroethylene). A 1-cm square window at the center of the lower and upper blocks allowed access of water vapor to the membrane. A BekkTech conductivity cell was also used to measure impedance data for comparison of two- and four-probe methods. BekkTech conductivity cell became commercially available at later stage of this research. The two-probe EIS technique (frequency range 1 Hz–1 MHz and AC voltage 10–50 mV) was employed using a Zahner IM6e potentiostat. Experimental impedance data were analyzed with ZSimpWin Version 2.00 software (Princeton Applied Research) and an equivalent circuit $(R_1Q_1)(R_2Q_2)$ that is described in Impedance Analysis section.

Nafion 117 membrane was treated in the following manner: boil in 3 wt% hydrogen peroxide solution for one hour, rinse with deionized water (18 MΩ), boil in deionized water for one hour, boil in 0.5 M sulfuric acid solution for one hour, boil in deionized water, rinse with deionized water, boil in deionized water, and soak in deionized water at room temperature. In each step, temperature was monitored to prevent overheating of the membrane above the glass transition temperature of Nafion 117 (110°C).[6] Use of a rectangular punch of width 6 mm and length 15 mm ensured uniformity in dimensions of membrane sample. Average thickness of the membrane was obtained by measurements at several locations using a digital micrometer (Mitutoyo

Corporation). During conductivity measurement, time to equilibrate the membrane with the environment was determined by tracking the conductivity until conductivity showed no significant change. Typically, membranes attained equilibrium with water vapor in 48 hours and with liquid water in 24 hours.
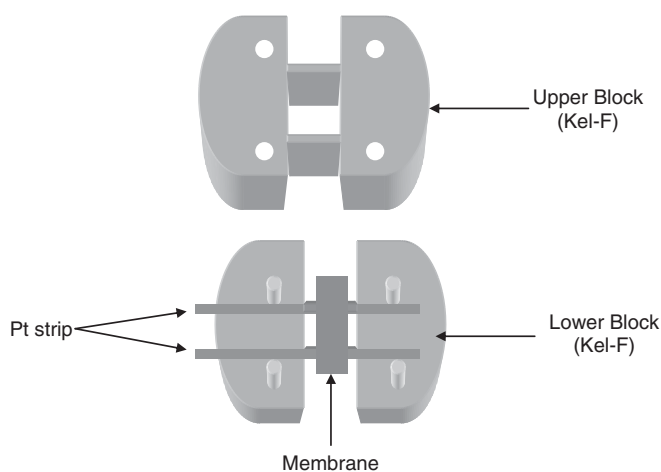
Figure 1. Schematic of in-plane conductivity cells. Typical membrane sample was 15-mm long and 6-mm wide. Width of platinum electrode strip was 1 mm for most studies.
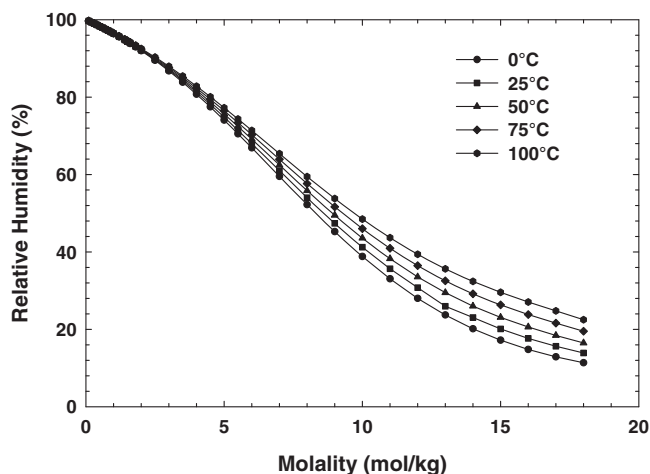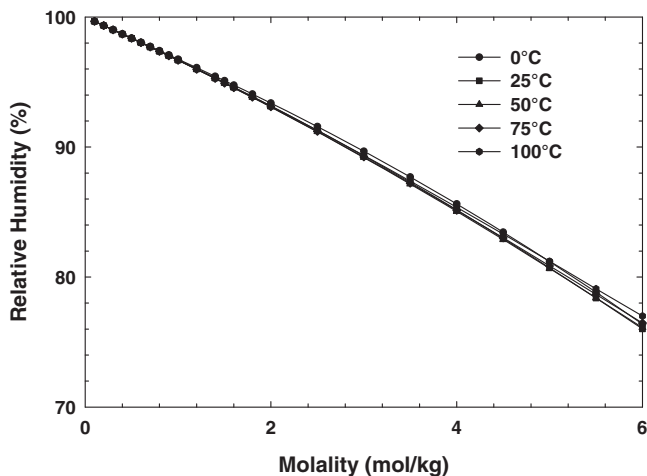
Figure 2. Calculated relative humidity in equilibrium with lithium chloride (LiCl) at various temperatures and salt molality from Eq. 1 using osmotic coefficient of lithium chloride salt.[29]

Water vapor sorption in the PEM is achieved by controlling the water vapor activity by means of salt solution. Percentage relative humidity %RH, as shown in Eq. 1, is 100 times the ratio of partial pressure of water, P^{vap}, to the vapor pressure of water, P^{sat}, both at system temperature T.[25] Water activity, a_w, is related to the relative humidity as shown in Eq. 1.[25] Eq. 1 describes the water activity and its relationship with salt molality.[25]

$$\%RH = 100\frac{P^{vap}}{P^{sat}} = 100 a_w = 100 \exp\left(-\frac{\phi_i^m M_s m_i \nu}{1000}\right) \qquad [1]$$

where ϕ_i^m is osmotic coefficient, ν is number of dissociated salt ions, m_i is salt molality, and M_s is solvent molecular weight. There are many organic and inorganic salts that can be utilized to control water vapor activity in a closed system.[24,26–28] For water vapor activity in the range of 0.10–1.0 and 0.75–1.0, lithium chloride and sodium chloride salts, respectively, are adequate in the temperature range of 25 to 80°C. We observed that water vapor activity in the range of 0.75–1.0 could be achieved in shorter time by sodium chloride salt than by lithium chloride salt.

In this work, we used lithium chloride salt for water vapor activity control in the range of 0.10–0.60, sodium chloride salt for water vapor activity control in the range of 0.75–0.85, and deionized liquid water for water vapor activity of 1.0. Figs. 2 and 3 were generated from

Figure 3. Calculated relative humidity in equilibrium with sodium chloride (NaCl) at various temperatures and salt molality from Eq. 1 using osmotic coefficient of sodium chloride salt.[30]
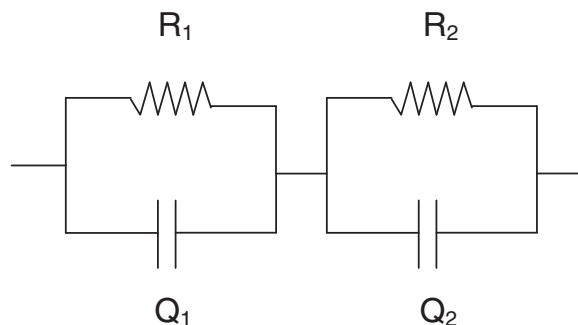
Figure 4. Equivalent circuit model.

Eq. 1 and osmotic coefficient data from literature.[29,30] As illustrated in Figs. 2 and 3, relative humidity increases with temperature and decreases with increase in salt molality. From Fig. 2, relative humidity from 10–100% can be achieved at any temperature between 0–100°C by varying the lithium chloride molality. Both sodium chloride salt and lithium chloride salt can control the high range of water vapor activity (Figs. 2 and 3). However, to decrease the measurement time in controlling the high range of water vapor activity, we used sodium chloride.

Results and Discussion

Impedance analysis.— The following expression describes the relationship between ionic conductivity (S cm^{-1}), resistance (ohm), and PEM dimensions (cm):

$$\sigma = \frac{L}{RA} \qquad [2]$$

where σ is ionic conductivity, R is ionic resistance, L is inter-electrode distance between voltage-sensing electrodes, and A is PEM area normal to current flow. In the in-plane configuration, PEM width w multiplied by thickness t is the PEM area normal to current flow ($A = wt$). In a typical Nyquist plot from a PEM, extrapolation of a semi-circle arc or low-frequency linear spectra to the X-axis gives the ionic resistance. Alternatively, an equivalent circuit is fit to the data to resolve the ionic resistance. In the present work, an equivalent circuit model $(R_1Q_1)(R_2Q_2)$ shown in Fig. 4 was fit to impedance data at all measurement conditions.

The equivalent circuit captures a system with two time-constants one for the PEM and the other for the interface. Inherently, resistor, R_1, in parallel combination with constant-phase element, Q_1, represents the impedance of PEM. Resistor, R_2, in parallel combination with constant-phase element, Q_2, represents the interfacial impedance. The constant-phase element captures the electrode surface roughness and system heterogeneity.[31] The impedance of a constant-phase element is given by $1/(Q^0(\omega j)^n)$ where Q^0 and n are frequency-independent parameters. The parameter n is 1 for ideal capacitor and varies between 0 and 1 for non-ideal capacitive elements. The equivalent circuit $(R_1Q_1)(R_2Q_2)$ can be resolved into real and imaginary parts to represent the equivalent impedance of the PEM and interface system.[32,33]

Through-plane and in-plane ionic conductivity.— Ideally, the through-plane ionic conductivity should be investigated. However, in through-plane ionic conductivity measurement by two- or four- or coaxial-probe method, the voltage-sensing electrode distance L (Eq. 2) is determined by the membrane thickness that typically varies from approximately 20 to 200 μm for commercial and candidate PEMs. Because of the PEM thickness acting as inter-electrode distance L, through-plane ionic resistance can vary only with electrode surface area A that is normal to ionic current flow. An in-plane conductivity cell configuration relative to through-plane configuration offers the spatial advantage because inter-electrode distance can be adjusted to obtain measurable in-plane ionic resistance.
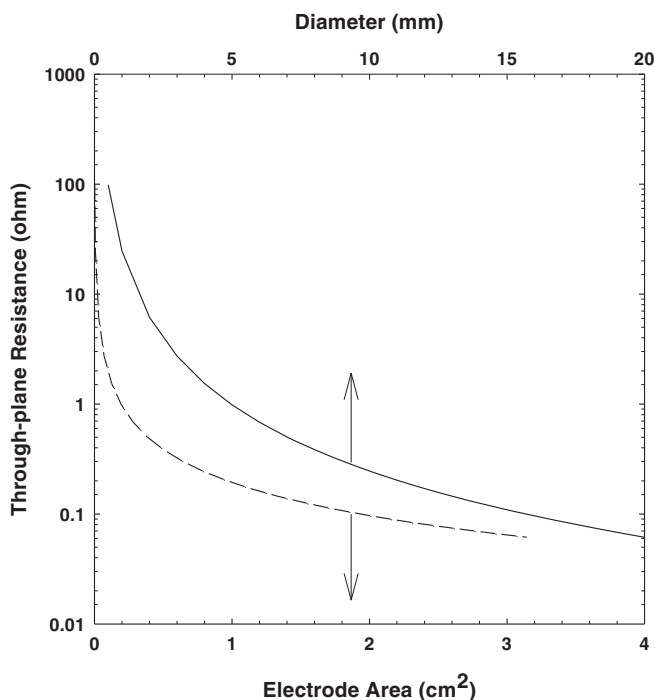
Figure 5. Calculated through-plane ionic resistance of membrane sandwiched between two co-planar electrodes using conductivity of 0.10 S cm^{-1} and membrane thickness of 200 μm. Membrane area is assumed to be identical to electrode area.

Figure 6. Impedance spectra for 1- and 10-mm wide Pt-strip electrodes of identical length. Impedance was recorded at 25°C and relative humidity of 100% in the frequency range of 1 MHz–1 Hz.
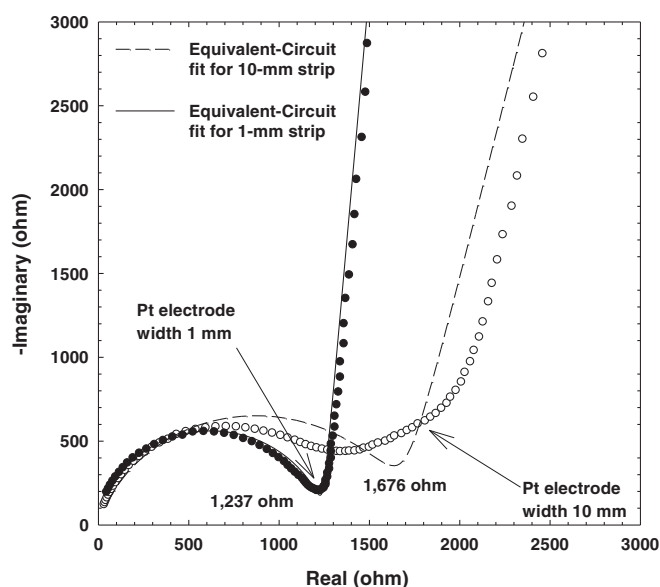
For fixed value of the ionic conductivity, Fig. 5 shows the variation of through-plane ionic resistance with electrode circular surface area A using a conductivity of 100 mS cm^{-1} and a 200 μm thick membrane. The calculated $R_{Through-plane}$ shown in Fig. 5 assumes a circular shape of the membrane of the same diameter as the two identical electrodes.

In through-plane configuration, theoretically, electrode surface area can be reduced or enlarged to any extent. However, dimensions of the PEM can influence the current distribution on the electrodes. For identical area of electrodes and PEM, current distribution is uniform on the electrodes. However, current distribution will become non-uniform if the membrane has a larger surface area than the electrode. Non-uniform current distribution will affect the ionic resistance measurement.

Increasing the electrode surface area can reduce the ionic resistance to such a low value that can be practically challenging to interpret from impedance spectra. For example, increasing the electrode diameter from 1 to 5 mm reduces the ionic resistance from 100 to 1 ohm which would be more difficult to measure by the EIS technique. Depending on convenience, a suitable contact area between PEM and electrodes might be employed to obtain measurable ionic resistance by the EIS technique with two- or four- or coaxial-probe method.

Effect of electrode dimension.— In impedance measurement by EIS technique, a non-uniform current distribution occurs at the PEM-electrode interface with large area because of PEM deformation from applied compressive force and water uptake. Applied compressive force can hinder water transport resulting in PEM deformation and surface heterogeneity. The two-probe EIS technique can display the non-uniform current distribution behavior that arises from physical deformation and surface heterogeneity at PEM-electrode interface. In a Nyquist plot from the two-probe method, distortion in impedance spectra is a signature of non-uniform current distribution. This distortion in the impedance spectra can lead to misinterpretation of the data.

Uniform presence of water throughout the PEM can improve current distribution and attenuate the distortion in the impedance spectra. Small contact area at PEM-electrode interface can improve the cur-

rent distribution and attenuate the distortion in the impedance spectra. Small contact area can improve water-transport at the PEM-electrode interface that can improve current distribution and produce artifact-free impedance spectra. In the conductivity cell used in this work, a narrow Pt strip electrode has advantages in providing small contact area that can reduce physical deformation and surface heterogeneity at PEM-interface. In this work, 1- and 10-mm wide Pt strips electrodes were employed to study the effect of electrode dimensions on impedance spectra in the through plane mode.

Fig. 6 shows the impedance spectra of Nafion 117 using the two-probe EIS technique with 1- and 10-mm wide electrodes at 25°C and 100% relative humidity. The semi-circle portion of the impedance spectra represents the resistance in parallel combination with the PEM capacitance. Distortion in impedance spectra in the low-frequency range is evident for the 10-mm wide electrode and is attributed to non-uniform current distribution. Extrapolation of the semi-circle arc or linear region to the real-axis in order to obtain ionic resistance can be challenging to interpret. An equivalent circuit $(R_1Q_1)(R_2Q_2)$ fit to the impedance data gave an ionic resistance of 1,237 ohm for 1-mm wide electrode and 1,676 ohm for 10-mm wide electrode that is higher by 26% from the 1-mm wide electrode. Reduction in Pt strip width from 10 to 1 mm attenuates the distortion in impedance spectra. Fig. 6 shows that use of 1-mm wide Pt electrode in the two-probe method is preferred. In the data reported here, 1-mm wide electrode was used to measure Nafion 117 conductivity for improved accuracy.

Capacitive behavior of polymer electrolyte membranes.— Polymer electrolyte membranes exhibit capacitive as well as ionic behavior because of water-uptake, and interaction between ionic groups and water. PEMs under dry condition, such as Nafion 117, have very low conductivity and dielectric constant.[19,20] However, water-uptake in PEMs transforms their ionic and dielectric properties. The EIS technique has been employed mostly to study ionic conductivity of PEMs. However, impedance data from the EIS technique can be interpreted to extract effective capacitance. Eq. 3 shows the expression for impedance of constant-phase element and Eq. 4 shows the expression for capacitance.[31–33]

$$Z(\omega)_{CPE} = \frac{1}{Q^0(j\omega)^n} \qquad [3]$$
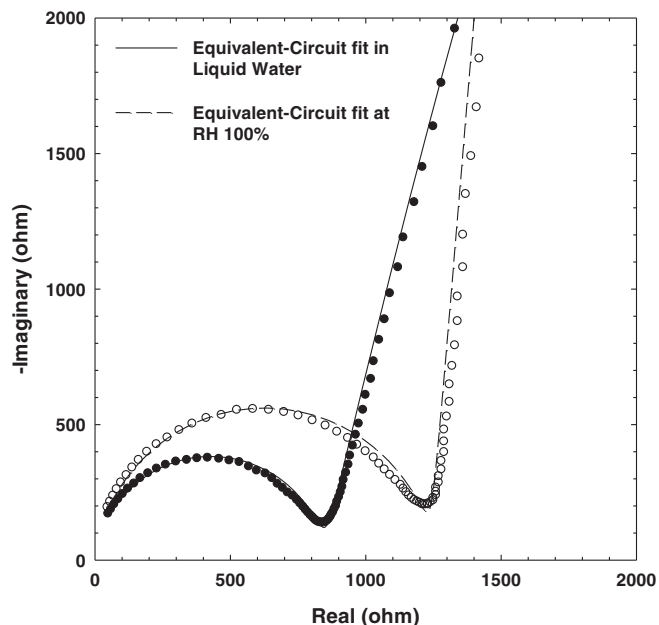
Figure 7. Impedance of Nafion 117 at 25°C and in frequency range of 1 MHz–1 Hz.

$$C_{Membrane} = \left[(Q^0)^{1/n} R^{\frac{1-n}{n}} \sin\left(\frac{n\pi}{2}\right) \right] \text{ at } \omega_{max} \qquad [4]$$

where ω_{max} is frequency at which the imaginary value of the PEM impedance reaches a maximum. If frequency-independent parameters Q^0 and n are known by fitting an equivalent circuit, Eq. 4 can be applied to obtain the capacitance of PEM.[33]

Fig. 7 presents a Nyquist plot for Nafion 117 at RH 100% and in liquid water, and it illustrates the effect of change in ionic resistance and capacitance at high-water content from liquid water and low-water content from water vapor at 100% relative humidity. For fixed dimensions of a PEM, the change in shape and size of impedance spectra indicates a change in the time-constant (RC). As shown in Fig. 7, the maximum in the absolute value of the imaginary impedance of Nafion 117 changed from 557 to 377 ohm due to change in water-content from water vapor at 100% relative humidity to liquid water. As shown in high-frequency region of the impedance spectra, a change in the imaginary part of PEM impedance is consistent with a change in dielectric constant of Nafion, as reported by Paddison et al.[19] Fig. 7 also shows the capability of the equivalent circuit $(R_1Q_1)(R_2Q_2)$ to fit impedance data at the two measurement conditions.

Fig. 8 shows the results of specific capacitance (Farad/g of dry membrane) that was obtained from Eq. 4, and Table II shows the fitted parameters corresponding to Fig. 8. Increase in water-uptake in Nafion 117 from 100% relative humidity to liquid water increases the specific capacitance by 10% from 58 to 64 nF/g. This increase in capacitance is consistent with an increase in dielectric constant of Nafion 117 due to a change in water uptake from water vapor to liquid water, as reported by Paddison et al.[19] Despite an increase in water uptake, Fig. 8 shows that the specific capacitance decreases with water vapor activity. This apparent contrary behavior is attributed to a change in volume of the membrane that is typically difficult to measure when membranes are assembled in a conductivity cell and are under a controlled environment.

Two- and four-probe methods.— The four-probe method can separate the interfacial from the membrane impedance, and it is advantageous for systems with high-interfacial impedance. However, the four-probe method requires more sophisticated equipment and selecting a certain frequency range is typically necessary to produce artifact-free
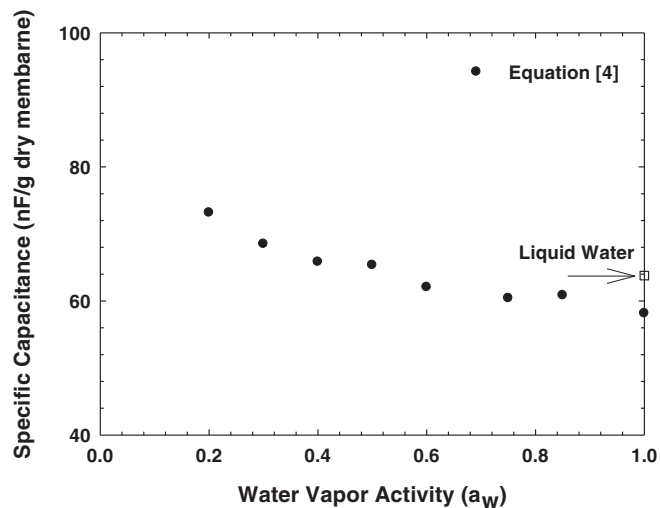
Figure 8. Specific capacitance (nF/g) of Nafion 117 membrane with water vapor activity. Capacitance was calculated from Eq. 4.

impedance spectra. The two-probe method is relatively suitable to apply for systems with intermediate and high-ionic impedances.
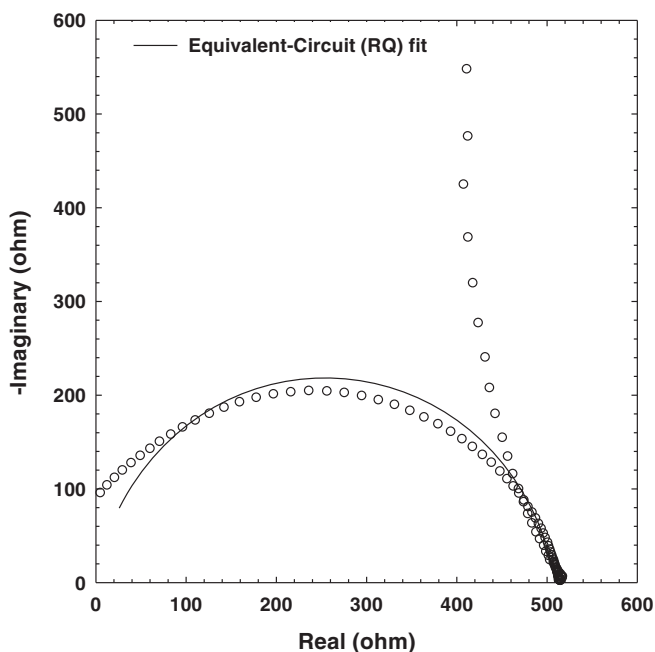
Fig. 9 shows the impedance spectra of Nafion 117 that was obtained from the four-probe method using a BekkTech conductivity cell (BekkTech), which was used for comparison of two- and four-probe methods. In fitting the equivalent circuit (RQ) for ionic conductivity calculation, we ignored the low-frequency impedance data (<60 Hz) to remove the artifact effect from interfacial contact of voltage-sensing electrodes and the PEM. In this work, Nafion 117 conductivity from a four-probe method ($82 \pm 1\%$ mS cm^{-1}) and the two-probe method ($79 \pm 1\%$ mS cm^{-1}) in water and at room temperature are statistically indistinguishable.

Nafion 117 conductivity.— Nafion 117 conductivity was measured at various relative humidities (10–100%) and temperatures (25–80°C) that encompass PEM fuel cells operating conditions. The two-probe EIS technique, in-plane configuration, and 1-mm wide electrode for improved accuracy was employed. No significant difference between machine direction and transverse direction of ionic conductivity was observed. Ionic conductivity increases with water-content and temperature. Nafion 117 has reasonable conductivity at high-relative humidity, but it is low at dry conditions. Fig. 10 illustrates the ionic conductivity behavior with relative humidity and temperature. At 25°C, ionic conductivity increases from 0.33 to 68 mS cm^{-1} for relative humidity from 10 to 100% and at other temperatures, ionic conductivity displays a similar qualitative trend. This increase in ionic conductiv-

Table II. Values of Circuit Parameters for Fig. 7.

| Parameters	Liquid Water	RH 100%
R_1 (ohm)	8.43×10^2	1.24×10^3
Q_1^0 (S s^n)	2.61×10^{-9}	2.27×10^{-9}
n_1	9.29×10^{-1}	9.31×10^{-1}
R_2 (ohm)	8.34×10^4	2.77×10^7
Q_2^0 (S s^n)	1.05×10^{-6}	3.58×10^{-7}
n_2	8.60×10^{-1}	9.48×10^{-1}
ω_{max} (Hz)	1.99×10^5	1.59×10^5
L (cm)	1.10×10^0	1.00×10^0
w (cm)	6.00×10^{-1}	6.00×10^{-1}
t (cm)	2.05×10^{-2}	2.00×10^{-2}
σ (S cm^{-1})	1.06×10^{-1}	6.74×10^{-2}
C_{PEM} (pF) (Eq. 4)	9.63×10^2	8.78×10^2

Figure 9. Nafion 117 impedance spectra by four-probe method in liquid water at room temperature and in frequency range of 1 MHz–1 Hz.

ity from 10 to 100% relative humidity shows that water uptake has enormous effect on ionic conductivity. At any relative humidity, ionic conductivity increases by minimum two times for temperatures from 25 to 80°C. Ionic conductivity in liquid water is about two times higher than that at 100% relative humidity.

A correlation for Nafion 117 conductivity was developed to calculate ionic conductivity as function of water vapor activity (0.1–1.0) and temperature (25–80°C). The following expression shows the ionic conductivity correlation.

$$\sigma(a_w, T) = (0.6877 + a_w)^3 \exp\left(-\frac{E_a}{RT}\right) \qquad [5]$$

$$E_a = 10440 a_w^{-1/4} \; \mathrm{J\,mol^{-1}}$$
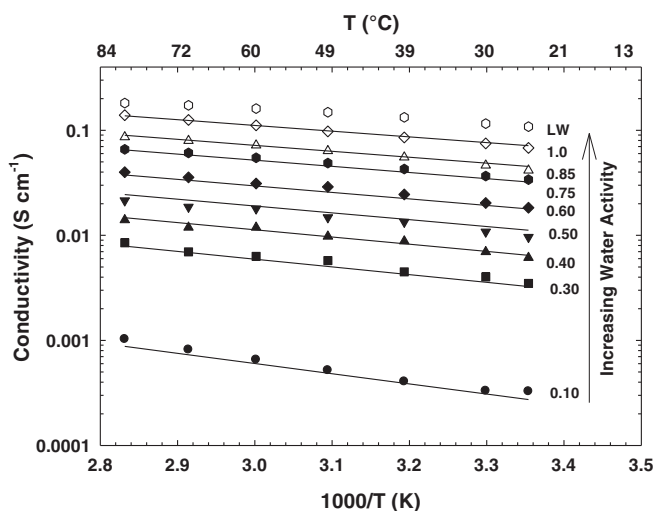
Figure 10. Nafion 117 conductivity as a function of temperature from 25 to 80°C. Symbols represent experimental results and solid lines represent results calculated from Eq. 5. LW stands for liquid water.
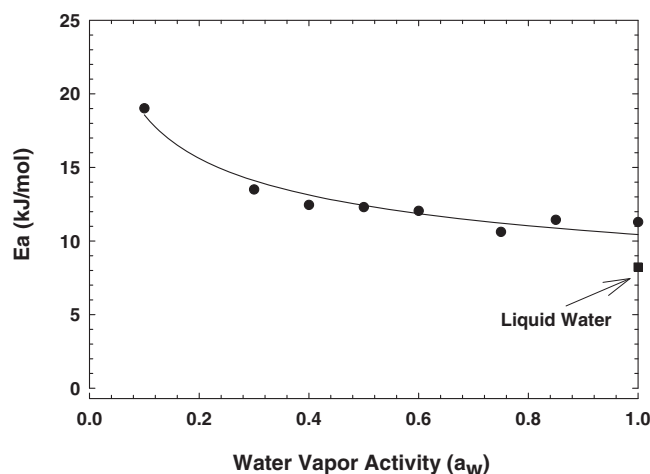
Figure 11. Activation energy of Nafion 117 ionic conductivity from Figure 10. Solid line shows the best fit of activation energy according to Eq. 5.

where σ is ionic conductivity (S cm^{-1}), a_w is water vapor activity, and *T* is temperature in Kelvin and *R* is universal gas constant (8.314 J K^{-1} mol^{-1}). The correlation shows that proton activation energy is dependent on water vapor activity. Fig. 10 shows that the calculated ionic conductivity agrees well with experimental results. The correlation captures the trend of ionic conductivity with temperature and relative humidity.

Nafion 117 conductivity follows Arrhenius behavior with temperature, as shown in Fig. 9. At a fixed relative humidity, the activation energy for proton transport was constant with temperature from 25 to 80°C. However, Fig. 11 reveals that activation energy varies with water activity. Activation energy decreased by 42% for water activity from 0.1 to 1 (19 to 11 kJ mol^{-1}). Activation energy further decreased by 27% for change in water-content from 100% relative humidity to liquid water.

Conclusions

An equivalent-circuit model is adequate to fit two-probe impedance data of a PEM across a spectrum of temperature and RH conditions. In the two-probe method in an in-plane measurement, a reduction in contact area at PEM-electrode interface improves the current distribution resulting in less distorted impedance spectra and a clearer interpretation of ionic resistance. Water-uptake in PEM influences capacitance leading to change in shape and magnitude of PEM impedance spectra with humidity. Two- and four-probe methods produce comparable conductivity if artifacts in impedance spectra are removed. Nafion 117 conductivity is strongly related to water-content and temperature. Conductivity increases with both temperature and water-content, with the latter having a greater influence. A correlation is presented that calculates conductivity at any water vapor activity and temperature. Activation energy of proton transport depends on water-uptake. High water-uptake reduces energy barrier for proton transport resulting in low-activation energy.

Acknowledgments

References

1. T. Soboleva, Z. Xie, Z. Shi, E. Tsang, T. Navessin, and S. Holdcroft, *J. Electroanal. Chem.*, **622**, 145 (2008).

2. J. Halim, F. N. Buchi, O. Haas, M. Stamm, and G. G. Scherer, *Electrochim. Acta*, **39**, 1303 (1994).
3. A. V. Anantaraman and C. L. Gardner, *J. Electroanal. Chem.*, **414**, 115 (1996).
4. N. Walsby, S. Hietala, S. L. Maunu, F. Sundholm, T. Kallio, and G. Sundholm, *J. Appl. Polym. Sci.*, **86**, 33 (2002).
5. J. J. Sumner, S. E. Creager, J. J. Ma, and D. D. DesMarteau, *J. Electrochem. Soc.*, **145**, 107 (1998).
6. Y. Sone, P. Ekdunge, and D. Simsonsson, *J. Electrochem. Soc.*, **143**, 1254 (1996).
7. M. Doyle, M. E. Lewittes, M. G. Roelofs, S. A. Perusich, and R. E. Lowrey, *J. Membr. Sci.*, **184**, 257 (2001).
8. R. F. Silva, M. DeFrancesco, and A. Pozio, *J. Power Sources*, **134**, 18 (2004).
9. P. C. Rieke and N. E. Vanderborgh, *J. Membr. Sci.*, **32**, 313 (1987).
10. M. J. Park, K. H. Downing, A. Jackson, E. D. Gomez, A. M. Minor, D. Cookson, A. Z. Weber, and N. P. Balsara, *Nano Lett.*, **7**, 3547 (2007).
11. K. Miura, J. O. Hong, K. Yashiro, Y. Nigara, T. Kawada, and J. Mizusaki, *Transaction of Material Research Society, Japan*, **26**, 1079 (2001).
12. T. A. Zawodzinski, Jr., C. Derouin, S. Radzinski, R. J. Sherman, V. T. Smith, T. E. Springer, and S. Gottesfeld, *J. Electrochem. Soc.*, **140**, 1041 (1993).
13. C. H. Lee, H. B. Park, Y. M. Lee, and R. D. Lee, *Ind. Eng. Chem. Res.*, **44**, 7617 (2005).
14. S. Ma, Z. Siroma, and H. Tanaka, *J. Electrochem. Soc.*, **153**, A2274 (2006).
15. H. L. Lin, T. L. Yu, and F. H. Han, *J. Polym. Res.*, **13**, 379 (2006).
16. G. Alberti, M. Casciola, L. Massinelli, and B. Bauer, *J. Membr. Sci.*, **185**, 73 (2001).
17. T. A. Zawodzinski, T. E. Springer, J. Davey, R. Jestel, C. Lopez, J. Valerio, and S. Gottesfeld, *J. Electrochem. Soc.*, **140**, 1981 (1993).
18. M. Merechal, J. L. Souquet, J. Guindet, and J. Y. Sanchez, *Electrochem. Commun.*, **9**, 1023 (2007).
19. S. J. Paddison, D. W. Reagor, and T. A. Zawodzinski, Jr., *J. Electroanal. Chem.*, **459**, 91 (1998).
20. Z. Lu, G. Polizos, D. D. Macdonald, and E. Manias, *J. Electrochem. Soc.*, **155**, B163 (2008).
21. T. A. Zawodzinski, Jr., M. Neeman, L. O. Sillerud, and S. Gottesfeld, *J. Phys. Chem.*, **95**, 6040 (1991).
22. G. Blumenthal, M. Cappadonia, and M. Lehmann, *Ionics*, **2**, 102 (1996).
23. J. R. Atkins, C. R. Sides, S. E. Creager, J. L. Harris, W. T. Pennington, B. H. Thomas, and D. D. DesMarteau, *J. New Mater. Electrochem. Syst.*, **6**, 9 (2003).
24. ASTM International, Designation E104-02, Standard Practice for Maintaining Constant Relative Humidity by Means of Aqueous Solutions, 1–3.
25. J. M. Prausnitz, R. N. Lichtenthaler, and E. G. de Azevedo, *Molecular Thermodynamics of Fluid Phase Equilibria*, 3rd ed., Chapter 9, p 512, Equations 9-11a, Prentice Hall PTR, New Jersey (1999).
26. J. F. Young, *J. Appl. Chem.*, **17**, 241 (1967).
27. P. H. Huang and J. R. Whetstone, Proc. Int. Symp. 1985, 577–596, Publisher ISA, RTP, NC, USA.
28. L. Greenspan, *J. Res. Natl. Inst. Stan. Technol.*, **81**, 89 (1977).
29. H. F. Gibbard, Jr. and G. Scatchard, *J. Chem. Eng. Data*, **18**, 293 (1973).
30. H. F. Gibbard, Jr., G. Scatchard, R. A. Rousseau, and J. L. Creek, *J. Chem. Eng. Data*, **19**, 281 (1974).
31. M. E. Orazem and B. Tribollet, *Electrochemical Impedance Spectroscopy*, Chapter 13, p 234, John Wiley & Sons, New York, (2008).
32. X. Z. Yuan, C. Song, H. Wang, and J. Zhang, *Electrochemical Impedance Spectroscopy in PEM Fuel Cells*, Chapter 4, p 141–148, Springer London Dordrecht Heidelberg Limited, New York (2010).
33. M. R. S. Abouzarri, F. Berkemeier, G. Schmitz, and D. Wilmer, *Solid State Ionics*, **180**, 922 (2009).